magnetic field in the proximity of the singular points where $B_{TOT} = 0$. The depth of their penetration and of the penetration of the fluxes between 0.22 MeV and 0.97 MeV linearly interpolated has been computed by the use of the values of atmospheric pressure and temperature valid for the month of December at a latitude of 70° (Houghton, 1979, p. 175) – see table II – and by the use of the values of the stopping power supplied by Dalgarno (1961) – see table III. The result is presented in fig. 10. Consequently, the specific power loss in terms of W/kg borne by those fluxes in the region between 100 and 85 km height was computed with the value of ρ, the air density, deduced with the formula $\rho = Mp/RT$, being $M = 28.9$ and $R = 8.314$, and with the use of a magnification factor equal to $8 \cdot 10^5$. Whence does this magnification factor come about? From the funneling action of the magnetic funnels formed around the singular points in the magnetosphere where $B_{TOT} = 0$.

The lines of flux of the magnetic field, as can be seen in fig. 1, converge as they approach the Earth's surface and in so doing guide and converge the energetic particles that arrive from the sun at the input of the funnel. At the equinoctial times the magnification will be the same for the two hemispheres, but at solstices the winter magnification will be significantly larger than that of the summer, as can be deduced by a glance at the sketch in fig. 1. Any effect that can be related to the funneling of the geomagnetic field will be stronger in the winter than in the

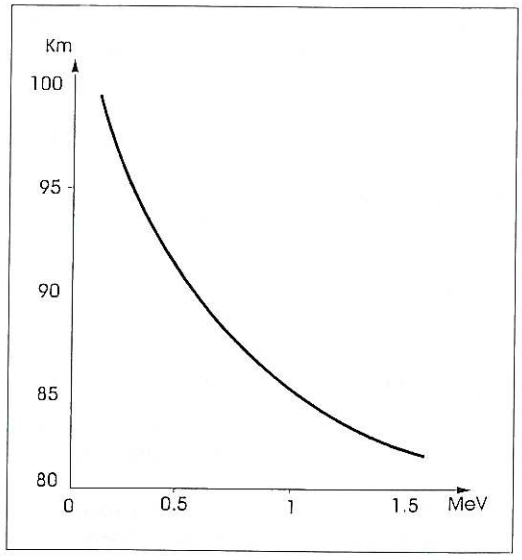

Fig. 10. Depth of penetration of low energy protons.

Table II. Model atmosphere. After Houghton (1979): *The Physics of Atmospheres* (Cambridge University Press), p. 175.

Geopotential height (km)	Pressure (mb) 70°N	Temperature (K)
80	$0.680 \cdot 10^{-2}$	214
85	$0.306 \cdot 10^{-2}$	215
90	$0.138 \cdot 10^{-2}$	217
95	$0.640 \cdot 10^{-3}$	219
100	$0.297 \cdot 10^{-3}$	215
105	$0.138 \cdot 10^{-3}$	212

Table III. Stopping power of air for protons. After Dalgarno (1961): Charged particles in the upper atmosphere, *Ann. Géophysique*, **17**, p. 36.

Incident energy (keV)	Stopping power (eV cm^2 10^{15})
20	29.0
30	31.0
40	33.0
50	34.3
60	35.4
70	35.8
80	35.8
90	35.6
100	35.0
150	32.0
200	28.4
300	25.4
500	16.8
1000	10.8
5000	3.3
10000	1.9

summer. For the winter, the magnification in the meridian plane will be given by the ratio between the segments AB and lm in fig. 1. In fact, the computation was split into two steps. As a first step the ratio AB/LM was read out of fig. 1 in its original dimensions, where the Earth's radius = $r_e \approx r_l \approx r_m = 1$ cm before the reduction imposed by the publication process; namely AB/LM = 2.5/0.4 = 6.25. Moreover, $\sin\theta_L = 4/6.5 = 0.6154$, $\theta_L = 37.98°$; $\sin\theta_M = 4.2/6.5 = 0.6462$, $\theta_M = 40.25°$. Hence, as a second step the ratio LM/lm was obtained by the use of the formula $r = C\sin^2\theta$, which is proper to an undisturbed, single dipole. Such a use is justified by the fact that the contribution of the mirror dipole on the magnetic field strength at points L and M, and a fortiori at points l and m, is negligible at a first approximation. We obtained

$$C_L = 6.5\,r_e/0.3787 = 17.16\,r_e$$
$$\sin^2\theta_l = 1/17.16 = 0.0583$$
$$\sin\theta_l = 0.2414$$
$$\theta_l = 13.97°$$

$$C_M = 6.5\,r_e/0.4175 = 15.57\,r_e$$
$$\sin^2\theta_m = 1/15.57 = 0.0642$$
$$\sin\theta_m = 0.2534$$
$$\theta_m = 14.68°$$

$$\theta_m - \theta_l = 14.68° - 13.97° = 0.71°$$
$$\overline{0.71°} \equiv 0.0124 \text{ rad}$$
$$\overline{lm} = 0.0124\,r_e.$$

The magnification factor in the meridian plane turns out to be equal to

$$(2.5/0.4) \cdot (0.4/0.0124) = 201.61.$$

The magnification factor in the east-west direction in the absence of the solar wind will be: $12\,r_e/1\,r_e = 12$, since $r_A \approx r_B \approx 12\,r_e$.

The increment of this value, namely 12, produced by the intervening solar wind is estimated as follows. Let AB/A′B′ be the ratio between the separation of the geomagnetic lines of flux (in the meridional plane) departing from points l and m, when they reach a distance from the Earth's center of about $12\,r_e$ in the presence of solar wind, and the separation of the same lines of flux in the absence of solar wind. A′B′ can be computed with the help of the relation $r = C\sin^2\theta$. Once AB/A′B′ is determined, it is induced that the same increment applies to the east-west direction rather than the north-south direction. We have that

$$r_{A'} = 12.5\,r_e = 17.16\,r_e \sin^2\theta_{A'}$$
$$\sin^2\theta_{A'} = 12.5/17.16 = 0.7284$$
$$\sin\theta_{A'} = 0.8535$$
$$\theta_{A'} = 58.59°$$

$$r_{B'} = 12.0\,r_e = 15.57\,r_e \sin^2\theta_{B'}$$
$$\sin^2\theta_{B'} = 12.0/15.57 = 0.7707$$
$$\sin\theta_{B'} = 0.8779$$
$$\theta_{B'} = 61.39°$$

$$\theta_{B'} - \theta_{A'} = 61.39° - 58.59° = 2.80°.$$

Hence $\overline{A'B'}^2 = 144 + 156.25 - 2 \cdot 150 \cdot 0.999 = 0.5500$ and $\overline{A'B'} = 0.7416$. Then AB/A′B′ = 2.5/0.7416 = 3.37. Hence, the magnification factor in the east-west direction, when solar wind is present, is estimated to be: $12 \cdot 3.37 = 40.44$. Altogether, the magnification factor of the «magnetic funnel» is thought to be $\approx 8 \cdot 10^3$. The specific loss suffered by the energetic protons between 0.16 MeV and 12.5 MeV of January 21, 1976 is found to be between $5.5 \cdot 10^{-2}$ W/kg and $7 \cdot 10^{-2}$ W/kg in the heights range between 105 km and 98 km, between $7 \cdot 10^{-2}$ W/kg and $6 \cdot 10^{-2}$ W/kg in the heights range between 98 km and 96 km, between $6 \cdot 10^{-2}$ W/kg and $4.5 \cdot 10^{-2}$ W/kg in the heights range between 96 km and 92 km, between $4.5 \cdot 10^{-2}$ W/kg and $2 \cdot 10^{-2}$ W/kg in the heights range between 92 km and 88 km, and drops to negligible values down below.

2.2.3. The amount of, say, $6 \cdot 10^{-2}$ W/kg, can be compared with the dissipation of $7 \cdot 10^{-3}$ W/kg which, according to Greenhow (1959), is the ratio of viscous dissipation of turbulent kinetic energy as could be deduced by the diffusion of visual meteor trails, the former being almost one order of magnitude larger than the latter. Hence, the landing of what we have called the «super» solar wind – like that observed on January 21, 1976 – on the polar atmospheric layer at about 96 km of altitude produces a significant increase in the coefficient of

eddy viscosity and a perturbation of the flow of the polar vortex which is known to exist at that altitude.

How does it come about? The incoming particles acting on a parcel of air in hydrostatic equilibrium would produce a vertical displacement in Δz in the atmosphere where the vertical gradient of temperature is dT/dz. Starting from the equation of motion, namely $\frac{\partial \underline{v}}{\partial t} = \frac{-\Delta p}{\rho} + \underline{g}$ (where $\underline{v}$ is the velocity, p is the pressure and $\underline{g}$ is the acceleration of gravity) and remembering that $dp = -gdz$, $\rho = Mp/RT$, $p = p_0 \exp\left\{-\int_0^z \frac{dz}{H}\right\}$ and $H = RT/M\rho$ (where M = molecular mass and R = gas constant per mole) we obtain the equation:

$$\Delta \ddot{z}\left(\frac{g}{T}\right)\cdot\left(\frac{dT}{dz}+\Gamma_d\right)\Delta z = 0 \qquad (2.7)$$

where Γ_d is the adiabatic lapse rate of temperature (Houghton, 1979, p. 7). The solutions of eq. (2.7) are the so-called gravity waves, *i.e.* the oscillations of the atmosphere under the influence of gravity, at an angular frequency $\omega_B = \left[\frac{g}{T}\cdot\left(\frac{dT}{dz}+\Gamma_d\right)\right]^{\frac{1}{2}}$ called the Brunt-Vaisala frequency. At 100 km height the period of the Brunt-Vaisala oscillations is about 60 s (Hines, 1960).

The alternate velocity of the waves, w' – while the average value, $\bar{w}$, is equal to zero- enhances the preexisting Reynold stress, which assumes the form, $\left(\frac{1}{\rho}\right)\cdot\frac{\partial(\rho\overline{u'w'})}{\partial z}$, u' being the variation of the horizontal component of the velocity. The Reynold stresses operate as frictional forces and slow down the circulation of the air of the polar vortex. In analogy with the molecular viscosity, it is possible to write $-\overline{u'w'} = K\left(\frac{\partial \bar{u}}{\partial z}\right)$ with $\bar{u}$ the average value of the horizontal velocity. The total expression of the Reynold stress in the horizontal direction (Houghton, 1979, p. 105) is

$$\left(\frac{1}{\rho}\right)\cdot\left[\frac{\partial(\rho\overline{u'u'})}{\partial x}+\frac{\partial(\rho\overline{u'v'})}{\partial y}+\rho K\frac{\partial^2 \bar{u}}{\partial z^2}\right]. \qquad (2.8)$$

The preexistence of turbulence (Greenhow, 1959) guarantes that $\frac{\partial^2 \bar{u}}{\partial z^2} \neq 0$. The advent of the gravity waves operates as an increase in K, that on account of the ratio $6 \cdot 10^{-2}/7 \cdot 10^{-3} \approx 9$ of the dissipated powers, can be estimated to be about thrice the value in absence of the gravity waves. In the present context, that involves averaging processes, it is important to point out that the period of the gravity waves near 100 km height, as recalled above, is about 60 s, while, as shown by Greenhow (1959), the time constant of the small eddy turbulence is of the same order of magnitude, namely 30 s at 90 km height.

It might even be estimated that a gram of air with a horizontal velocity of 20 m/s, having a kinetic energy of 0.200 J, under the action of such Reynold stresses for half an hour could be reduced almost to a full stop. If, for example, the power of $6 \cdot 10^{-5}$ W/g over half an hour is spent just to slow down the motion of the gram of air, the energy of the gram of air will be reduced to 0.092 J. But even the dissipated 0.108 J will work against the linear energy of the gram of air, so that a dramatic reduction of its original speed could be envisaged. Could a parcel of air moving with a velocity of 20 m/s at 100 km height be kept under the action of the predicted Reynold stresses for half an hour? The rotational velocity of the air at 100 km height, at 76° of latitude and at $v = 0$ would be 113 m/s. When $v = 20$ m/s its rotational velocity would be 93 m/s. The width of the terminal mouth of the «magnetic funnel» is $2 \cdot \overline{\text{lm}} = 160$ km. It will be swept in 1720 s. Furthermore, it must be added that any slow down imposed on a section of the polar vortex will be partially transferred and accumulated in the following sections. Then it is possible to conclude that the influx of the «super» solar wind can strongly perturb the flow of the polar vortex at altitudes between 90 and 100 km in the polar region.

Experimental evidence appears to support the above findings. According to Rees *et al.* (1979) «High ionospheric absorption in Spain is associated with disruption of the normally strong winter vortex around a warm winter mesospheric pole».

2.2.4. The consequences of the disruption of the polar vortex can be understood when the principle of conservation of potential vorticity is recalled (Houghton, 1979, p. 96). It states that

$$d_h \cdot \frac{\left[\frac{(\zeta + f)}{h}\right]}{dt} = 0. \qquad (2.9)$$

where d_h/dt denoted $\frac{\partial}{\partial x} + \frac{\partial}{\partial y}$; ζ = the vorticity; $f = 2\Omega\sin\phi$ is the Coriolis term which depends on Ω the rotating velocity of the Earth and on the latitude ϕ and h = the vertical width of the fluid vorticity. The quickest way of presenting the significance of eq. (2.9) is to quote directly from Houghton: «Equation (2.9) is a simplified statement of the conservation of potential vorticity. It has important consequences for the atmospheric flow. Consider, for instance, adiabatic flow over a mountain barrier. As a column of air flows over the barrier its vertical extent decreases so that ζ must also decrease. A westward moving airstream will, therefore, move equatorward as it passes over the barrier». «For easterly flow the air must begin to move southward before it reaches the mountain barrier». We are not dealing with a mountain barrier, but with a barrier represented by the stopped vortex between 92 and 100 km height. Even in our case an equatorward moving airstream will ensue at the heights between, say, 82 and 92 km.

The existence of a horizontal transport from high latitudes to medium latitudes is consistently suggested in the literature as a cause of winter anomaly events. In an exhaustive study by Arnold and Krankowsky (1979) on mid-latitude ionosphere structure and composition measurements during winter, after the presentation of the enhanced concentration of NO experimentally observed during winter anomaly, it is stated: «Possible causes of mesospheric nitric oxide enhancement could be an increased downward transport or a meridional transport of auroral nitric oxide» and again «meridional transport of nitric oxide originated at high latitudes may have contributed to the NO-enhancement». Similar statements can be found in the papers of the following authors: Offermann (1979), Offermann *et al.* (1979) and Labitze *et al.* (1979). Moreover, Rees *et al.* (1979), in discussing the relation between the local dynamical structure of the atmosphere and the ionospheric absorption during the Western European Winter Anomaly Campaign 1975/1976, point out that: «After being predominantly northward above 30 km and southward at lower altitudes before 30 December 1975, the meridional component (of the wind) moderated and then become southward at all altitudes. Peak velocities of the order of 40 m/s near 70 km coincided with several days of very high absorption (L_d) between 2 and 7 January and including the first rocket salvo of 4 January. A temporary decrease in the A3 absorption (L_0) between 8 end 13 January coincided with a return to northward winds above 60 km with a maximum of 40 m/s near 90 km. Subsequently, the long period of high absorption between 14 and 27 January recorded variable southward winds from ground level to nearly 90 km, with variable maxima between 20 and 40 m/s». According to these authors, it is also true that: «Near 90 km altitude, the phase of the wind variability was inverted with respect to that below 85 km». But «at 95 km a high correlation between southward meridional wind and high absorption (L_d) was obtained». We do not emphasize the role of the inverted wind direction near 90 km, as was done in the abstract and in the summary of the quoted paper, because we attribute the observed warmth of the polar mesosphere to the influx of the «super» solar wind rather than to the convergence toward the winter pole of a transported NO.

2.2.5. The meridian transport of the arctic (antarctic) air toward the equator produces an accumulation at low latitudes of NO of auroral origin. There the nitric oxide is ionized by the

intense Lyman-alpha radiation from the sun. This effect can be seen from two points of view. First the Lyman-alpha radiation penetrates down to about 80 km height because it is not absorbed by O_2, O, N_2, $O_2(^1\Delta_g)$, H and He gases, which are characterized by relatively high ionization potentials corresponding to wavelengths smaller than the 121.6 nm of the Lyman-alpha (Ratcliffe, 1972, p. 39). Second, the ionization potential of NO is 9.3 eV (Bortner, 1963, p. 63), which corresponds to a wavelength of 133.4 nm, larger than 121.6 nm. Arnold and Krankowsky (1979) detected densities of NO over Spain during winter anomaly events of the order of $3 \cdot 10^{13} m^{-3}$ between 80 and 90 km. The figure has to be compared with the value of $1 \cdot 10^{12} m^{-3}$ (Whitten and Poppoff, 1965, p. 70) for quiet conditions. The enhancement is one order of magnitude, just that required to explain the enhancement of the corresponding observed electron densities (Widdel *et al.*, 1979). In turn, this enhancement of the electron density is that required to generate the observed radio wave absorption during winter anomaly (Rees *et al.*, 1979).

Hence, the sequence of events analyzed in the Subsections 2.2.1 to 2.2.5 appears sufficient to explain the genesis of a winter anomaly event. Once this explanation is accepted, it must be concluded that the winter anomaly is necessarily a winter phenomenon.

Offermann *et al.* (1982) in their scale analysis of the data obtained during the Western European *D*-Region Winter Anomaly Campaign bring about an operational model called «the inverted chimney». It is interesting to note that the mode of operation proposed and illustrated in the preceding paragraphs is similar to that of the «inverted chimney». Indeed, in both models the air with a content of NO is first pushed down and then deviated sidewise. Nevertheless, there is a difference between the two. The «inverted chimney» is supposed to be operative at a low latitude, where the anomaly is taking place, while our scheme is supposed to become operative at polar latitudes where the polar vortex rotates, and is a consequence of the application of the principle of conservation of potential vorticity to a perturbed polar vortex. The transfer of the air with a content of NO to lower latitudes will follow.

Offermann *et al.* (1982) in their paper advance some doubts on the effective existence of meridional transport. First, because the absence of any dynamic forcing implies the absence of equatorward motions; second, because an equatorward motion of an air front will result in a dilution of NO due to the increasing circumference of the latitude circles; third, because the circulation analysis performed by Labitzke *et al.* (1979) up to an altitude of 80 km did not reveal such a transport. But in our scheme a dynamical forcing is present: it is represented by the momentum of the deviated polar vortex. Also, this kind of jet will not undergo a dilution in its motion toward the equator. Also the work of Labitzke *et al.* (1979) does not extend above 80 km where the core of the jet is supposed to advance. Furthermore, under the hypothesis of the model proposed in the preceding paragraphs the so called magnetic funnel remains fixed in space, while the underlying Earth rotates in an anticlockwise motion. Then the nozzle of the magnetic funnel, from which the energetic particles emerge to produce a stop and hence a deviation equatorwards of the flux of the pole vortex, appears to be continuously receding to an observer located in the Earth's ionosphere. Such an observer will have the impression that the jet of the deviated polar vortex arrives from a northwest direction. This is what Labitzke *et al.* (1979) found and is reported in their table 1, reproduced here under the heading of table IV.

With regard to the study on the transport of NO in the *D*-region during winter anomaly by Garcia *et al.* (1987), it is important to notice that the boundary conditions on which their model is based are opposite to those we have proposed. The geopotential height at the bottom of the atmosphere, namely at 100 mbar (16 km), is given as the starting point. The elaborated treatment of the problem is interesting because it illustrates the possible role of stationary and travelling planetary waves in the production of the winter anomaly. The conclusions reached are in agreement with the conclusion of our analysis concerning the important role of the transport of NO from the auroral zone to lower latitudes where the anomaly materializes. But while we envisage a decreasing intensity of the

Table IV. Advection and absorption. After Labitzke *et al.* (1979): Planetary waves in the strato-and mesosphere during the Western European Winter Anomaly Campaign 1975/1976 and their relation to atmospheric absorption, *J. Atmos. Terr. Phys.*, **41**, p. 1160.

ARANGIUEZ – BALERMA (AB)			
Large scale circulation	Date	Absorption (dB)	
Advection from northwest	31 Dec. 1975	High	+ 15
Advection from northwest	28 Jan. 1976	Excessive	+ 28
Strong wind from WNW	6 Jan. 1976	Excessive	+ 26
Advection from northeast	4 Feb. 1976	Low	+ 1
Advection from northwest	13 Jan. 1976	High	+ 13
Advection from northwest	21 Jan. 1976	Moderate	+ 6

anomaly as the lower latitudes are approached, on account of the increasing dispersion of the jet originated by the disturbed solar vortex, the results of Garcia *et al.* (1987) present a situation where there is not a monotonous decrease of the anomaly with a decreasing latitude, but a rather patchy wavelike distribution is obtained. The two contrasting models are not mutually exclusive. In the analysis of the practical case that in general is rather complex, it will be advisable to bear in mind both of them and the superposition of their effects. In the case of the Western European Winter Anomaly Campaign it seems that the model of our proposal prevails. Indeed, fig. 2 of the paper of Friedrich *et al.* (1979) relative to that Campaign shows an increasing anomaly with increasing latitude.

A different position is taken by the paper on the winter anomaly by Rapoport and Sinel'nikov (1998). These authors are concerned with some experimental work carried out at Volgograd during the years 1979-1990. After excluding the transport of NO downward from higher regions of the thermosphere or upward from the lower stratosphere as the mechanism responsible for the production of the anomaly, they come to the conclusion that NO should come from the auroral zone. Since meridional transport of NO from polar regions, where NO is abundant, to lower latitudes cannot be expected to take place spontaneously, because it would be opposite to the prevailing wind on the winter season, they see in the observed displacement of the wintry circumpolar cyclonic vortex the origin of the meridian shift of NO. Their scheme, though different, is quite similar to ours.

3. General conclusions

The anomalous winter anomaly whereby the winter ionization in the lower *D*-region of the ionosphere is less than should be expected was explained with the help of fig. 5. Such a figure – from Störmer – shows that the trajectories of ionized energetic particles entering the magnetic field of a simple dipole are confined in a well delimited space. Outside of this space is the so-called forbidden region. In dealing with the case of a magnetic field like that of fig. 1 we have implicitly implied that fig. 11 should take the place of fig. 5. Our fig. 11 was obtained by the combination of two graphs like that of fig. 5, one displaced along the axis with respect to the other and then rotated. The axis marked EE indicates the equatorial plane. In our case, the energetic particles must be seen as entering first the space delimited by the line AA and afterwards the space delimited by the line DD, the transition from one space to the other being indicated by one of the transverse dashed lines. When the transition takes place on the line labeled I, the energetic particles from the space delimited by AA will be deposited in the space delimited by DD all on the right side of EE or, in other words, in the summer hemisphere. If in addition to what has been said the constant γ, which characterizes the incoming particles as half of their moment of the momentum in the direction normal to EE, has values between (– 0.920) and (– 0.9285), then the particles will land in the lower *D*-region of space DD again in the summer hemisphere according to the quoted demonstration of Störmer. The process just de-

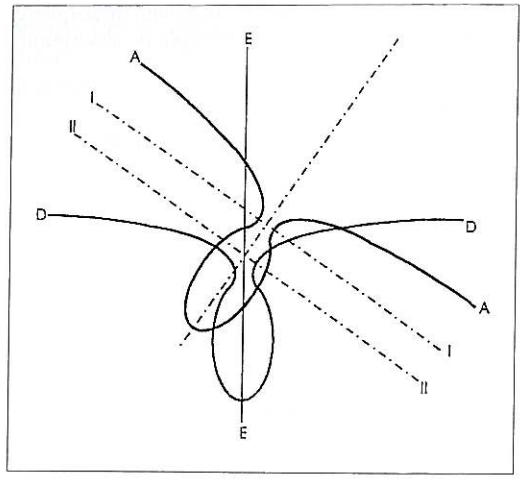

Fig. 11. Boundary between the allowed region and the forbidden region for the trajectories of ionized energetic particles moving in a field as that fig. 1.

scribed leads us to conclude that there would be a lack of ionization in the winter lower *D*-region. When the transition takes on the line labeled II no hemispheric anisotropy will materialize. All the passages indicated in this paragraph have been supported in Subsection 2.1 by numerical computations.

A completely different approach was taken to explain how the standard winter anomaly can be generated. A sequence of events was shown to offer an interconnection, at least on a particular instance, between the geomagnetic field slantly compressed by the solar wind as sketched in fig. 1 and the increase in the radio wave absorption at some relatively low latitudes. The presence of what has been called a magnetic funnel, located on the winter side of the deformed geomagnetic field, was shown to give a crucial contribution to the process under examination. The immission into the magnetic funnel of what has been indicated as a super solar wind represents a necessary ingredient of the entire development. The consequent slowing down of the polar vortex and the ensuing equatorward displacement of the polar air with its content of NO of auroral origin was evidenced. NO with its low ionization potential was seen to be responsible for the enhancement of the upper *D*-region ionization. Then the anomaly we are referring to seems to reside in the solar activity. The proposed explanation of the genesis of winter anomaly has two probatory aspects: not only does it definitely connect the phenomenon with the winter season, but it also justifies its longitudinal anticorrelation, since the equatorward motion of the air produced by the slowing down of the polar vortex will ensue when this slowing down is limited to a finite range of longitudes. This result can also be ascribed to the fact that the Earth's polar axis is not coincident with the geomagnetic dipole's axis, hence making the rotation of the nozzle of the magnetic funnel that conveys the energetic protons not concentric with the polar vortex.

At this stage of the analysis, it is impossible to advance any serious hypothesis on the mechanism that might induce a materialization of the super solar wind. Nevertheless, in this direction, it is noteworthly that, during the Western Europe Winter Anomaly Campaign 1975/1976, the radio wave absorption recorded noon peaks on January 7, 14, 21 and 28 (Widdel *et al.*, 1979). Moreover according to Shapley and Beynon (1965) a study of the day-to-day variation of ionospheric absorption carried out in connection with the winter anomaly shows that: «there is frequently a tendency for maxima to recur at intervals of about 5-8 days, and in the present limited sample of data it so happens that this recurrence tendency averaged out at exactly 7 days». Then it is worth quoting from Ratcliffe (1972, p. 14): «The spiral magnetic field – of the sun – is often divided into four or six sectors of roughly equal size, such that in the neighboring ones the field is directed in opposite senses as shown in fig. 1.5. The sectors rotate with the sun so that at the Earth there are four or six reversals of the field during each solar rotation. The sectors are formed gradually and often persist for many solar rotations». Figure 1.5 of Ratcliffe is reproduced here as fig. 12. It is also known that the solar synodic period of rotation is 27 days at the equator and that the sun rotates faster near the equator and more slowly towards the poles (Skilling and Richardson, 1954, p. 134).

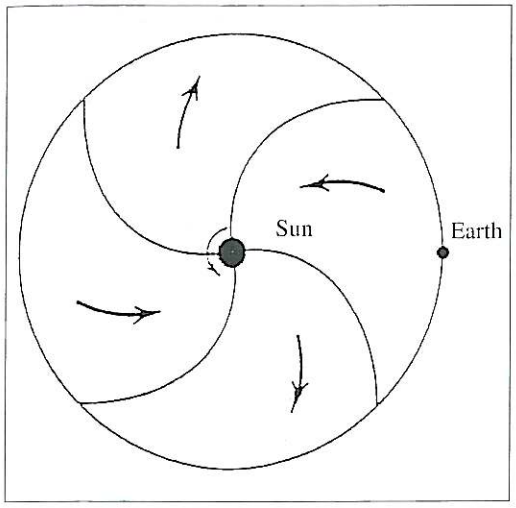

Fig. 12. The solar magnetic field carried radially outwards by the solar wind, which assumes a spiral form because the sun is rotating. After Ratcliffe (1972): *An Introduction to the Ionosphere and Magnetosphere* (Cambridge University Press), fig. 1.5.

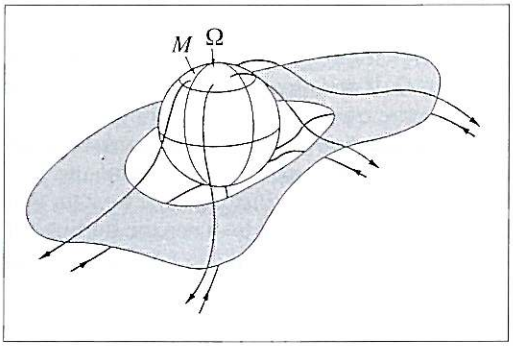

Fig. 13. Three-dimensional sketch of the equatorial heliospheric current sheet. After Smith *et al.* (1978): *J. Geophys. Res.*, **83**, p. 723.

Figure 13, from Smith *et al.* (1978), illustrates how the solar magnetic field leaves the sun and enters the interplanetary space. Along the plane of the sun's magnetic equator a thin current sheet, the heliospheric current sheet, separates the sun's magnetic field of the two hemispheres. Above and below that sheet the open field lines run parallel to each other. That sheet is not plane, but has a wavy shape because of the angle between the rotation axis and the magnetic axis of the sun and of a quadrupole moment in the solar magnetic field. The Earth, which is located on the plane of the ecliptic, sees alternatively fields of opposite polarity as the sun rotates. The wavy shape of the heliographic current sheet determines the existence of the magnetic sectors of fig. 12. More frequently 4 sectors are present, but at times 6 sectors are observed according to Smith *et al.* (1978).

The super solar wind is guided by the magnetic lines of force of the sun that are shaped as indicated in figs. 12 and 13 by the outflow of the regular solar wind. According to fig. 13 the super solar wind lands on the heliographic current sheet from both sides to assume a laminar shape. Hence, it moves in the interplanetary space along the spiral lines of fig. 12. The super solar wind will then reach the Earth only if it moves in the plane of the ecliptic. This condition will be achieved whenever the supporting heliographic sheet is intersected by the plane of the ecliptic, that is at the root of the boundary between two sectors. Hence, the branches of spirals that are traced in fig. 12 represent the paths of the super solar wind that reaches the Earth. As the sun rotates with a Synodic period of, say, 28 days, the Earth would be swept, when the sectors are 4, every 28/4 = 7 days or every ~ 5 days when the sectors are 6. Just as it was experimentally observed as indicated above. Then, our explanation of the genesis of winter anomaly, which was based on a single event, can find the support of a larger number of similar events.

Until now nothing has been said about the fact that the winter anomaly phenomenon is associated with a warming of the stratosphere. Some comments on this subject will be here presented since some further support to our interpretation of the genesis of the winter anomaly can be gathered. On this subject, the current literature presents some conflicting statements. According to Rees *et al.* (1979), for example, the enhancement of the radio wave absorption follows the stratospheric warming, with a time delay of about 2-4 days, suggesting that the winter anomaly is a consequence of the stratospher-

ic perturbation. Shapley and Beynon (1965) when looking for the possible phase difference between the stratospheric and ionospheric phenomenon found, for example, that at the end of November 1961 the onset of the winter anomaly was followed some three days later by a significant increase in the stratospheric temperature.

It seems possible to prove that the contradiction between these different sets of data is only apparent. Let us introduce the working hypothesis, hence with no experimental or theoretical support for the moment, that the stratospheric heating is produced by the arrival in the Earth's atmosphere of an electromagnetic beam of radiation emitted by the sun, concurrently with the super solar wind. (A synchrotron radiation from the heliospheric current sheet: only that part which lies in the plan of the ecliptic, when in its rotation it shows up from behind the sun? – Then, «concurrently» because their origins would be simultaneous, but a quadrant apart). A discussion of the possible genesis of such an e.m. beam of radiation will be deferred to another occasion. For brevity, as we proceed in our analysis, the e.m. beam of radiation will be called simply «the beam» and the super solar wind will be called simply «the jet». The situation resulting from our hypothesis is depicted in fig. 14. An observer located on the Earth, as the sun rotates, will receive the jet 2-4 days ahead or after the arrival of the beam. The beam could be seen to precede the jet or *vice versa*. This interpretation, given without considering the rotation of the Earth on its own axis, will be valid when δ_0, the time interval that separates two successive transits of the same event, is an even multiple of a half a day and t_0, the time that the jet takes to cover the distance sun-Earth, is also an even multiple of a half of a day. Otherwise, when $\delta_0 = (2n + 1)$ (day/2) and $t_0 = (2m + 1)$ (day/2) the observed sequence of events will be characterized by a period of $2\delta_0$ for the duo jet-first-beam-second; when $\delta_0 = (2n + 1)$ (day/2) and $t_0 = (2m)$ (day/2) the sequence of events will be characterized by a period of $2\delta_0$ for the duo beam-first-jet-second; and when $\delta_0 = (2n)$ (day/2) and $t_0 = (2m + 1)$ (day/2) the observer at a point of longitude, say, λ_0 (in the winter) will detect a series of single jets separated by an interval δ_0, while an observer

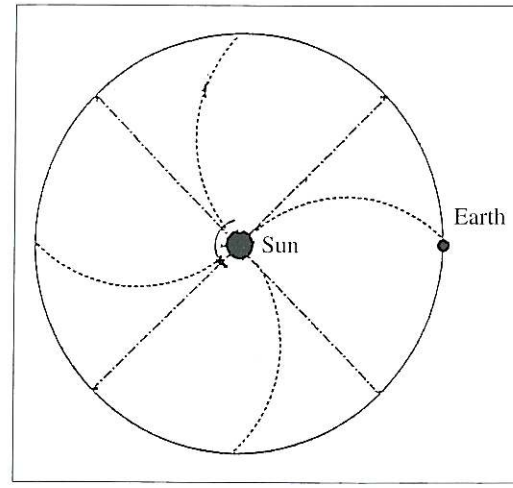

Fig. 14. ----- Traces of beams of ionized particles; —·— traces of hypothesized electromagnetic beams.

located on a point of longitude $(\lambda_0 + 180°)$ (in the winter) will detect a series of single beams separated by an interval δ_0. Table V supplies a comprehensive view of the four cases just discussed. Of course, a similar analysis should be carried out for any fraction of a day different from day/2. If during a campaign of observation one or more quantities involved in the process under examination change, the outlined sequences will be interrupted. On the basis of the presented considerations it is possible to state that there is no contradiction between the findings of Rees *et al.* (1979) and those of Shapley and Beynon (1965).

But the scheme of fig. 14 becomes a real key to the understanding of a long sequence of stratospheric warmings and enhancements of ionization in the upper *D*-region. We will utilize data obtained by Offermann *et al.* (1979) during the Western European Winter Anomaly Campaign. Reference is made to fig. 15 where a comparison of Channel 3000 infrared fluxes and A3 absorption is made possible. Infrared data are taken as a measure of atmospheric temperature at about 80 km height. The A3 data are diurnal averages and represent electron densities at 80-90 km height. These authors attach the following comments: «most of the strong peaks

Table V. Sequences of events.

Case 1: $\delta_0 = 2n$(day/2) $t_0 = 2m$(day/2)								
Time (days)	0	3	7	10	14	17	21	24
At long. l_0	beam	jet	beam	jet	beam	jet	beam	jet
At long. $l_0 + 180°$	–	–	–	–	–	–	–	–
Case 2: $\delta_0 = (2n + 1)$(day/2) $t_0 = (2m + 1)$(day/2)								
Time (days)	0	3.5	7.5	11	15	18.5	22.5	26
At long. l_0	–	jet	beam	–	–	jet	beam	–
At long. $l_0 + 180°$	beam	–	–	jet	beam	–	–	jet
Case 3: $\delta_0 = (2n + 1)$(day/2) $t_0 = 2m$(day/2)								
Time (days)	0	3	7.5	10.5	15	18	22.5	25.5
At long. l_0	–	–	beam	jet	–	–	beam	jet
At long. $l_0 + 180°$	beam	jet	–	–	beam	jet	–	–
Case 4: $\delta_0 = 2n$(day/2) $t_0 = (2m+1)$(day/2)								
Time (days)	0	3.5	7	10.5	14	17.5	21	24.5
At long. l_0	–	jet	–	jet	–	jet	–	jet
At long. $l_0 + 180°$	beam	–	beam	–	beam	–	beam	–

in A3 absorption in fig. 7 (fig. 15 for us) find their counterpart in temperature peaks». But there are days «when temperature is clearly high and nevertheless A3 absorption is low. There are 7 days of this kind, which are denoted by arrows in fig. 7 (fig. 15 for us)». «The interesting feature about the 7 days mentioned is that they are spaced very regularly at intervals of 7 days (and 14 days in one case). As they were Mondays, they will be called the 'Mondays' for brevity». According to the scheme of fig. 14 the temperature at about 80 km height is determined by the arrival of the e.m. beams, which proceed further and end in warming the stratosphere, and also by the arrival of the jet of ionized particles, which deposit their energy in the region between 90 and 80 km height and hence produce an increase in temperature moving equatorward and ending up with an increase in electron density. The days when the peak of temperature was accompanied by a peak of A3, *i.e.* electron density, were those of the arrival at the Earth of the jet of ionized particles. The days when the peak of temperature was accompanied by a minimum of A3, the so-called Mondays, were those of the arrival at the Earth of the e.m. beam. Note that even these days were separated by a 7 day interval in coherence with the scheme of fig. 14.

We have presented the strict, though quite hidden, correlation that exists between the sun and the Earth, because in such a frame our explanation of the genesis of the winter anomaly could find a stronger credibility, in spite of some crude approximations utilized throughout along our dissertation.

Finally, we evidence that the jets sketched in fig. 14 are portions of an Archimedean spiral.

Lines of force of the interplanetary magnetic field of the sun have been throughly analyzed by Parker (1958) who found that

$$\frac{r}{b} - 1 - \ln\left(\frac{r}{b}\right) = \frac{v_m}{b\omega}(\Phi - \Phi_0) \qquad (3.1)$$

where r and Φ are the spheric coordinates of a line with reference to the sun, b is the radial distance from the sun's center beyond which the solar gravitation and outward acceleration by high coronal temperature can be neglected, so that the outward velocity is a constant v_m. Fur-

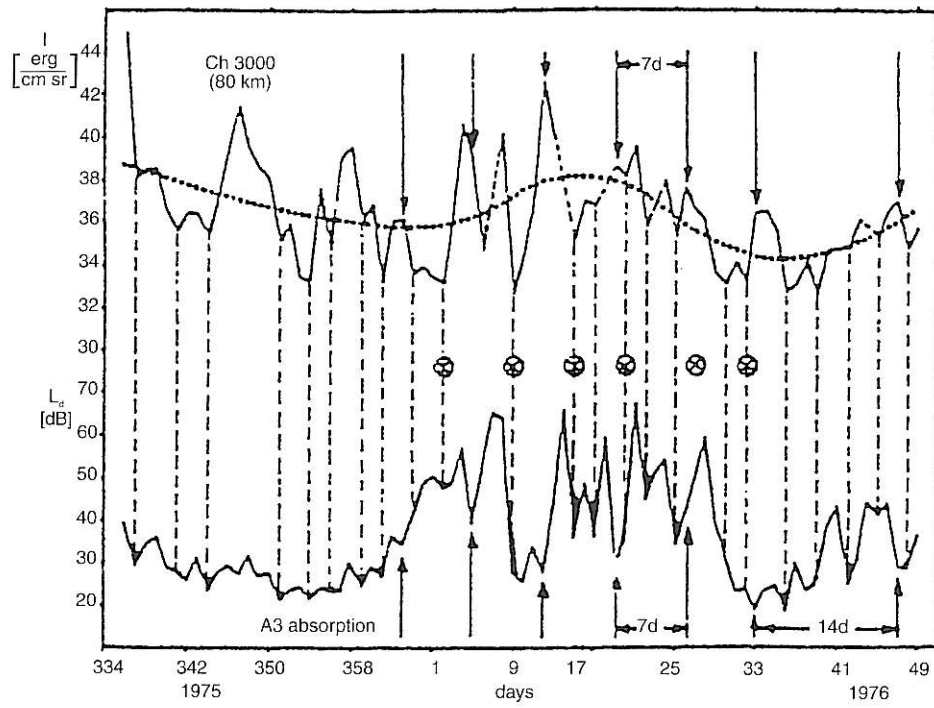

Fig. 15. Comparison of Channel 3000 infrared fluxes and A3 absorption. Infrared data are taken as a measure of atmospheric temperature at about 80 km. Diurnal averages of A3 data are given. They represent electron densities at 80-90 km. After Offermann *et al.* (1979): *J. Atmos. Terr. Phys.*, **41**, p. 1058.

thermore, $\Phi_0 = \Phi$ at b. The radius b is estimated to be of the order of 10^6 km. In comparison to the distance of the Earth from the sun, namely 150×10^6 km, the quantity b becomes negligible. For $b \cong 0$ and $\Phi_0 = 0$ the relation (3.1), being

$$\lim_{b \to 0} \left[b \ln\left(\frac{r}{b}\right) \right] = 0, \text{ becomes}$$

$$r \cong v_m \Phi / \omega \qquad (3.2)$$

that is an Archimedean spiral.

The particles of the jets are forced to follow such a spiral by the magnetic field embedded in the flow of the solar wind. Indeed, a particle of the solar wind emerging from a given point on the solar surface will move with a constant velocity, v_m, along a radial direction which emerges from the center of the sun and passes through that point. A continuous succession of directions will emerge from such a point as the sun rotates with a constant angular velocity ω. A continuous succession of particles will accompany the succession of those directions. Let us consider a sequence of particles emerging from a given point of the surface of the sun such that the first has just reached a point on the Earth's orbit and the last is just emerging from the solar surface. The difference of their age be the time t_0; the difference between their associated directions be $\theta_0 = \omega t_0$. The path distance between the sun and the Earth is the well known length L_0. Knowing L_0 and θ_0, we can deduce the value of $v_m = L_0 \omega / \theta_0$.

An imaginary observer located on a point of the Earth's orbit and operating with a clock and an imaginary optical instrument pointed toward the surface of the sun could measure either θ_0 or, if preferred, t_0. He can compute the value of v_m. This is what we can do after we are told that the

transit of a straight radius of fig. 14 precedes the transit of the stretch of an Archimedean spiral by a number of days, as the sun rotates and the Earth, at a first approximation, is thought to be at rest. The scientific literature reports an average delay between the two transits of 3 days.

Then, $v_m = \frac{1.5 \cdot 10^8}{3 \cdot 8.64 \cdot 10^4} = 579 \frac{\text{km}}{\text{s}}$. Since only a rough estimation of v_m is needed, the computation of v_m did not take into account the motion of the Earth and other minor effects. The figure of $579 \frac{\text{km}}{\text{s}}$ is in a good agreement with the values of the velocity of the solar wind observed by IMP 7 and IMP 8 and reported in fig. 4. Indirectly it lends support to our hypotheses.

Appendix

The Appendix is devoted to the determination of Γ, the coefficient of collisional detachment of electrons from negative ions (O_2^-), which plays an important role in the lower *D*-region of the ionosphere.

Its value can be obtained after a comprehensive analysis of the data reported in fig. 7.

They were gathered during the Western European Winter Anomaly Campaign 1975/1976 by Widdel *et al.* (1979).

We will start from the continuity equations that are valid for the lower ionosphere, namely

$$\frac{dN}{dt} = q - \alpha_D N N^+ - K n_0^2 N + \Gamma n N^- + \rho N^- \tag{A.1a}$$

$$\frac{dN^-}{dt} = -\alpha_i N^- N^+ + K n_0^2 N - \Gamma n N^- - \rho N^- \tag{A.1b}$$

$$N^+ = N + N^- \tag{A.1c}$$

where:

q = ionization rate;
N = electron density;
N^- = negative-ion density;
N^+ = positive-ion density;
α_D = ion-electron recombination coefficient;
α_i = ion-ion recombination coefficient;
K = 3-body attachment coefficient;
Γ = negative-ion collisional detachment coefficient;
ρ = negative-ion photodetachment rate;
n = neutral molecule density;
n_0 = oxygen molecule density.

Let $\lambda \equiv \frac{N^-}{N}$. Then the eqs. (A.1a,b,c) become

$$\frac{d\lambda}{dt} = K n_0^2 (1+\lambda) - [\rho + \Gamma n + N(\alpha_i - \alpha_D)]\lambda(1+\lambda) - \frac{\lambda q}{N} \tag{A.2a}$$

$$\frac{dN^-}{dt} = -\left(\alpha_i + \frac{\alpha_D}{\lambda}\right)(N^-)^2 + \frac{q\lambda}{(1+\lambda)} + \left[\frac{N^-}{(\lambda+\lambda^2)}\right] \cdot \frac{d\lambda}{dt} \tag{A.2b}$$

$$N^+ = (1+\lambda)\, N. \tag{A.2c}$$

Equation (A.2a) can be simplified since $K = 3 \cdot 10^{-42}$ m^6/s at the ambient temperature (Chanin *et al.*, 1959), $\rho = 0.44$ s^{-1}, $\alpha_D = 2 \cdot 10^{-13}$ m^3/s and $\alpha_i = 1.8 \cdot 10^{-13}$ m^3/s (Webber, 1962). Furthermore, at 60 km height $n = 5.37 \cdot 10^{-2}$ mol/m^3 (Houghton, 1979, p. 175) and hence $n_0 = 1.074 \cdot 10^{21}$ mol/m^3, $N \approx 0(10^8)$ electrons/m^3 and $q < 4 \cdot 10^{-1}$ electrons/m^3 s (Webber, 1962); at 40 km height $n = 7.42 \cdot 10^{22}$ mol/m^3 (Houghton, 1979, p. 175) and hence $n_0 = 1.48 \cdot 10^{22}$ mol/m^3, $N \approx 0(10^7)$ electrons/m^3 and $q < 5.10^5$ electrons/m^3 s (Webber, 1962). For Γ we will use the tentative value of $2.5 \cdot 10^{-23}$ m^3/s. Thus, eq. (A.2a) simplifies to

$$\frac{d\lambda}{dt} = Kn_0^2(1+\lambda) - [\rho + \Gamma n]\lambda(1+\lambda). \tag{A.3}$$

This is a Riccati equation which has the particular solution $u = \dfrac{Kn_0^2}{(\rho + \Gamma n)}$. Its general solution is

$$\lambda = u - \frac{\exp[-(Kn_0^2 + \rho + \Gamma n)\cdot t]}{\left\{\dfrac{(\rho+\Gamma n)\exp[-(Kn_0^2 + \rho + \Gamma n)\cdot t]}{(Kn_0^2 + \rho + \Gamma n)} + C\right\}} \tag{A.4}$$

where C depends on the initial conditions, when q changes from one condition to another. In order to estimate the recovery time for λ let us consider the limiting case that corresponds to $\lambda = 0$ when $t = 0$. Then $C = (\rho + \Gamma n)/u(Kn_0^2 + \rho + \Gamma n)$. Then, the λ will return to 9/10 of its steady state value, namely u, in an interval that is determinated by the following relation:

$$\frac{9}{10}\cdot u = u - \frac{\exp[-(Kn_0^2 + \rho + \Gamma n)\cdot t]}{\left\{\dfrac{(\rho+\Gamma n)\exp[-(Kn_0^2 + \rho + \Gamma n)\cdot t]}{(Kn_0^2 + \rho + \Gamma n)} + C\right\}}. \tag{A.5}$$

At 60 km of altitude, $Kn_0^2 = 3.50$ s^{-1}, $(\rho + \Gamma n) = 0.57$ s^{-1}, and $u = 6.14$; then eq. (A.5) yields the solution $t \approx 1$ s. At 40 km of altitude, $Kn_0^2 = 657$ s^{-1}, $(\rho + \Gamma n) = 2.295$ s^{-1}, and $u = 286$; then eq. (A.5) yields the solution $t \approx 11$ ms. Therefore, it can stated that at most a few seconds after the change of q (within the limits foreseeable for the low D-region) $d\lambda/dt = 0$, so that eq. (A.2b) can be restated as

$$\frac{dN^-}{dt} = -\left(\alpha_i + \frac{\alpha_D}{\lambda}\right)(N^-)^2 + \frac{q\lambda}{(1+\lambda)}. \tag{A.6}$$

This is again a Riccati equation that has the particular solution

$$u_1 = \left[\frac{q\lambda}{(1+\lambda)\left(\alpha_i \dfrac{\alpha_D}{\lambda}\right)}\right]^{\frac{1}{2}}.$$

Its general solution is

$$N^- = u_1 - \frac{2\exp\left[-2u_1\left(\alpha_i + \dfrac{\alpha_D}{\lambda}\right)t\right]}{\left\{\dfrac{\exp\left[-2u_1\left(\alpha_i + \dfrac{\alpha_D}{\lambda}\right)t\right]}{u_1} + C_1\right\}}. \tag{A.7}$$

From this expression the time of transition from the value of N^- pertinent to a given value of q to the value of N^- pertinent to a different value of q can be obtained with an approach similar to that discussed above in connection with the quantity λ. In the case of N^- the times of transition are of the order of hours. But now we will concentrate our attention on the steady state values of N^-, namely the u_1's.

We deduce that the data of fig. 7 are pertinent to steady state conditions. Under steady state conditions and only under steady state conditions the negative ions density can be expressed as the product of a function of λ and a function of q, namely

$$N^- = f_1(\lambda) \cdot f_2(q) = \left[\frac{\lambda}{(1+\lambda)\left(\alpha_i + \frac{\alpha_D}{\lambda}\right)} \right]^{\frac{1}{2}} \cdot (q)^{\frac{1}{2}}.$$

Under different steady state conditions relative to different q's, $f_2(q_1) \neq f_2(q_2)$, while $f_1(\lambda)$ does not change. We can interpret $f_2(q)$ as a modulated function of q *versus* the height h, while $f_1(\lambda)$ is its modulating function of λ *versus* h. In fig. 7 we have curves that are clearly relative to different rates of ionization, the data collected on January 21 and February 5 being pertinent to q's much larger that q's of the data collected on January 4, 6 and 28. But all these curves show a definite knee at the same altitude of 53 km. We take this evidence as a proof that we are confronted with steady state data.

With regard to the evidenced knee we will show that it can be used for the determination of Γ the coefficient of collisional detachment of N^-. The λ being always given by $Kn_0^2/(\rho + \Gamma n)$ for all the steady state conditions, the knee indicates that above 53 km the dependence of λ *versus* height, hence of N^- *versus* height, is more or less dominated by $\lambda = Kn_0^2/\rho$, as if $\rho > \Gamma n$, and that below 53 km the dependence of λ *versus* height, hence of N^- *versus* height, is more or less dominated by $\lambda = Kn_0^2/\Gamma n$, as if $\rho < \Gamma n$. In other words, the data of fig. 7 seem to indicate that at 53 km height $\rho = \Gamma n$. This leads to a determination of Γ in terms of $\Gamma = \rho/n = 0.44/1.35 \cdot 10^{22} = 3.26 \cdot 10^{-23}$ m^3/s. The value of n at 53 km height was deduced by the values of pressure and temperature valid for December at a latitude of 40° supplied by Houghton (1979, p. 175). It is worth pointing out that the deduced value of Γ is quite close to the tentative value of Γ utilized above. The determination of the coefficient of collisional detachment appears to be a quite valuable by-product of the precious data collected during the Western European Winter Anomaly Campaign 1975/1976.

With the newly found value of Γ it is possible to compute the values of the effective recombination coefficient, namely $\alpha_e = (1 + \lambda) \cdot (\alpha_D + \alpha_i \lambda)$. Computations led to the following results:

at 60 km	$\lambda = 5.63$	and	$\alpha_e = 8 \cdot 10^{-12}$	m^3/s
at 40 km	$\lambda = 230$	and	$\alpha_e = 9.6 \cdot 10^{-9}$	m^3/s.

These values of λ and α_e were used in Section 2.1.

REFERENCES

APPLETON, E.V. (1937): Regularities and irregularities in the ionosphere - I, *Proc. R. Soc. London, Ser. A*, **162**, 451-479.

ARNOLD, F. and D. KRANKOWSKY (1979): Mid-latitude lower ionosphere structure and composition measurements during winter, *J. Atmos. Terr. Phys.*, **41**, 1127-1140.

BORTNER, M.H. (1963): The chemical kinetics of atmospheric deionization, *Report R63SD34*, General Electric, pp. 88.

CHANIN, L.M., A.V. PHELPS and M.A. BIONDI (1959): Measurements of slow electrons in oxygen, *Phys. Rev. Lett.*, **2**, 344-346.

DALGARNO, A. (1961): Charged particles in the upper atmosphere, *Ann. Géophysique*, **17**, 16-49.

FRIEDRICH, M., K.M. TORKAR, G. ROSE and H.U. WIDDEL (1979): The seasonal variation of radio wave absorption in Europe, *J. Atmos. Terr. Phys.*, **41**, 1163-1170.

GARCIA, R.R., S. SOLOMON, S.K. AVERY and G.C. REID (1987): Transport of nitric oxide and the *D*-region winter anomaly, *J. Geophys. Res.*, **92**, 977-994.

GREENHOW, J.S. (1959): Eddy diffusion and its effect on meteor trails, *J. Geophys. Res.*, **64**, 2208-2209.

HINES, C.O. (1960): Internal atmospheric gravity waves at ionospheric heights, *Can. J. Phys.*, **38**, 1441-1481.

HOUGHTON, J.T. (1979): *The Physics of Atmospheres* (Cambridge University Press), pp. 203.

LABITZKE, K., K. PETZOLDT and H. SCHWENTEK (1979): Planetary waves in the strato-and mesosphere during the Western European Winter Anomaly Campaign 1975/1976 and their relation to atmospheric absorption, *J. Atmos. Terr. Phys.*, **41**, 1149-1162.

OFFERMANN, D. (1979): An integrated GBR campaign for the study of the *D*-region Winter Anomaly in Western Europe 1975/1976, *J. Atmos. Terr. Phys.*, **41**, 1047-1050.

OFFERMANN, D., P. CURTIS, J.M. CISNEROS, J. SATRUSTEGUI, H. LAUCHE, G. ROSE and K. PETZOLDT (1979): Atmospheric temperature structure during the Western European Winter Anomaly Campaign 1975/1976, *J. Atmos. Terr. Phys.*, **41**, 1051-1062.

OFFERMANN, D., H.G.K. BRÜCKELMANN, J.J. BARNETT, K. LABITZKE, K.M. TORKAR and H.U. WIDDEL (1982): A scale analysis of the *D*-region winter anomaly, *J. Geophys. Res.*, **87**, 8286-8306.

PARKER, E.N. (1958): Dynamics of the interplanetary gas and magnetic fields, *Astrophys. J.*, **128**, 664-676.

RAPOPORT, Z.TS. and V.M. SINEL'NIKOV (1998): Experimental electron concentration profiles of the midlatitude lower ionosphere and the winter anomaly, *Int. J. Geomagn. Aeron.*, **1** (2), 161-168.

RATCLIFFE, J.A. (1972): *An Introduction to the Ionosphere and Magnetosphere* (Cambridge Univ. Press), pp. 256.

REES, D., A.F.D. SCOTT, J.M. CISNEROS, H. WIDDEL and G. ROSE (1979): Relationship between the local dynamical structure of the atmosphere and ionospheric absorption during the Western European Winter Anomaly Campaign 1975/1976, *J. Atmos. Terr. Phys.*, **41**, 1063-1074.

SATO, T. (1980): Morphological features of the winter anomaly in ionospheric absorption of radio waves at middle latitudes, *J. Geophys. Res.*, **85**, 197-205.

SHAPLEY, A.H. and W.J.G. BEYNON (1965): «Winter Anomaly» in ionospheric absorption and stratospheric warming, *Nature*, **206**, 1242-1243.

SKILLING, W.T. and R.S. RICHARDSON (1954): *A Brief Text in Astronomy* (Henry Holt & Co.), pp. 327.

SMITH, E.J., B.T. TSURUTANI and R.L. Rosenberg (1978): Observations of the interplanetary sector structure up to heliographic latitudes of 16°: Pioneer 11, *J. Geophys. Res.*, **83**, 717-724.

Solar-Geophysical Data, 378 (Supplement), p. 54, February 1976, U.S. Department of Commerce (Boulder, Colorado, U.S.A. 80302).

Solar-Geophysical Data, 384 Part II, p. 9, August 1976, U.S. Department of Commerce (Boulder, Colorado, U.S.A. 80302).

STÖRMER, C. (1955): *The Polar Aurora* (Clarendon Press), pp. 403.

VELINOV, P. (1968): On ionization in the ionospheric *D*-region by galactic and solar cosmic rays, *J. Atmos. Terr. Phys.*, **30**, 1891-1905.

WEBBER, W. (1962): The production of free electrons in the ionospheric *D*-layer by solar and galactic cosmic rays and the resultant absorption of radio waves, *J. Geophys. Res.*, **67**, 5091-5106.

WHITTEN, R.C. and I.G. POPPOFF (1965): *Physics of Lower Ionosphere* (Prentice Hall, Inc.), pp. 232.

WIDDEL, H.U., G. ROSE, K. SPENNER, M. FRIEDERICH and K.M. TORKAR (1979): Electron densities during winter anomalous absorption of different intensity observed at 37.1°N, 6.73°W, during winter 1975/1976 - I, *J. Atmos. Terr. Phys.*, **41**, 1105-1119.

(received May 24, 2000;
accepted June 14, 2001)